Supporting Information

Bent Alkyne Units as Active Sites: Structure–Activity Correlation in Graphdiyne-Inspired Polymers for Photocatalytic Hydrogen Evolution

Xingzhong Wu[a,b], Jing Chen, [a,b] Jingyi He [a,b] , Qun Liu [a,b] and Yongjun Li*[a,b]

a. Beijing National Laboratory for Molecular Sciences (BNLMS), CAS Key Laboratory of Organic Solids, Institute of Chemistry, CAS Research/Education Center for Excellence in Molecular Sciences, Chinese Academy of Sciences, Beijing 100190, P. R. China.

b. University of Chinese Academy of Sciences, Beijing 100049, PR China.

*Corresponding author.

E-mail address: liyj@iccas.ac.cn (Y. Li)

1 Experiment Section

1.1 Materials

All reactions are performed under argon unless otherwise stated. Most of the chemical reagents were purchased commercially and used without further purification unless otherwise stated. Column chromatography was performed on silica gel (size 200-300 mesh).

1.2 Instruments

^{1}H and ^{13}C NMR spectra were recorded on a Bruker AVANCE 400 or Bruker AVANCE III 500WB instrument, at a constant temperature of 25°C. Chemical shifts are reported in parts per million from low to high field and referenced to TMS. Matrix-assisted laser desorption/ionization Fourier transform ion cyclotron resonance (MALDI-FT-ICR-MS) mass spectrometry were performed on a Bruker Solarix 9.4T FT-ICR-MS mass spectrometer. EI mass spectrometric measurements were performed

on a SHIMADZU GCMS-QP2010 pulse Spectrometer. Infrared spectroscopy was measured on a Bruker TENSOR-27 spectrometer. Raman spectra were recorded using an NT-MDT NTEGRA Spectra system, with excitation from an Ar laser at 473 nm. Solution UV–vis absorption spectra were recorded at room temperature on a Jasco V-570 spectrophoto-meter. Solution fluorescence emission spectra were recorded at room temperature on a Jasco FP-6000 spectrophotometer. XPS was performed using an ESCALab250Xi apparatus using PTEP transferred onto a glass slide. For the characterization of X-ray diffractometer (XRD), the PTEP was transferred onto a glass slide. The sample was characterized by XRD (Rigaku Dmax200, Cu Kα). The scanning rate was 2 °/min, and the 2θ range was from 2° to 30°. The morphologies of the as-prepared samples were examined using field emission scanning electron microscopy (FESEM, Hitachi S-8020) and TEM (HT7700, JEM-2100F). 1,4-diethynylbenzene was synthesized following the previously reported route. [S1],[S2]

Photocurrent measurements: The photocurrent measurements were performed using an electrochemical workstation (CHI660E) with a standard three- electrode photoelectrochemical cell, where the copper sheet coated with the PTEP sample, platinum wire and Ag/AgCl act as the working, auxiliary, and reference electrode, respectively. The electrodes were immersed in a sodium sulfate electrolyte solution (0.1 M, pH = 7.0), which was purged with N_2 for 30 min before the test. The working electrodes were prepared as follows: First, the copper sheet was washed in an ultrasonic bath with a 1 M hydrochloric acid (HCl) solution for 20 minutes. Then, it was rinsed sequentially with water and acetone, and placed in an argon environment. Next, 10 mg of TEP was dispersed in a mixed solution of chloroform (500 mL) and TMEDA (100 μL), and the copper sheet was added to this mixture. The reaction was carried out at 45°C for 72 hours. Finally, the copper sheet was taken out, rinsed with acetone, and dried. The photocurrent was measured at various bias voltages (vs. Ag/AgCl) with a 300 W Xe lamp by intermittent irradiation. The EIS spectra were recorded by applying a 10 mV AC signal in the frequency range from 100K to 0.01Hz at a DC bias of 0.3V vs. RHE (i.e. − 0.3V vs. Ag/AgCl). Current density was calculated using the exposed geometric surface area of 1.0 cm^2 of the photoelectrode

($J_{photocurrent\ density}$ =$J_{measured\ photocurrent}$/$S_{exposed\ geometric\ surface\ area}$)
The applied potential vs. Ag/AgCl is converted to RHE potential using the following equation:
E_{RHE} = $E_{Ag/AgCl}$ +0.059pH+$E^0_{Ag/AgCl}$($E^0_{Ag/AgCl}$ =0.199V)The applied potential vs. Ag/AgCl is converted to RHE potential using the following equation:
ERHE = $E_{Ag/AgCl}$ +0.059pH+$E^0_{Ag/AgCl}$($E^0_{Ag/AgCl}$ =0.199V)

Photocatalytic H_2: generation reactions were performed in a 100-mL closed Pyrex reactor with a quartz window under the visible light irradiation. In a typical photocatalytic reaction, 5 mg of a certain PTEP sample was ultrasonically dispersed in 20 mL aqueous solution of ascorbic acid (700 mg). Pt (0.5 wt %) was in-situ photodeposited on the PTEP surface as co-catalyst to boost H_2 generation. The suspension was purged with argon for 30 min to remove the residual air within the reactor prior to reaction. A 300 W Xe lamp ((PLS-SXE300D, Beijing Perfect light) with optical cutoff filter (λ≥420 nm) was used as the visible light source for the photocatalytic reactions. The reactant solution temperature was maintained at 8 ℃ during the reaction using flow from a cycle cooling water system. The amount of hydrogen produced was determined by gas chromatography (Agilent, GC-7890B) using a thermal conductivity detector (TCD), with argon as the carrier gas. The Apparent Quantum Yield (AQY) was calculated using the following formula:

$$AQY\ (\%) = \frac{N_e \times K}{N_p} = \frac{v \times N_a \times K \times h \times c \times 10^9}{I \times A \times t \times \lambda} \times 100\%$$

Photoluminescence (PL) Spectroscopy: Steady-state PL spectra, PL decay spectra and PL quantum yield were measured on the FLS980 fluorescence spectrometer. The wavelength range for detection was 410nm - 850 nm. PL decay spectra were measured by time-correlated single-photon counting with an excitation wavelength of 405 nm, and the decay curves were fitted to obtain the average fluorescence lifetimes

τ_{ave} = 0.314 ns (0.2127ns 89.30 Rel%, 1.11567ns 10.70 Rel%). QY = 0.85%

The radiative (k_r) and nonradiative (k_{nr}) recombination rates of excitons in the PTEP sample were calculated based on the results of QY and fluorescence lifetime using the following formula:

$$\tau_{ave} = 1/(k_r + k_{nr})$$

$$QY = k_r/(k_r + k_{nr})$$

The final values obtained were: radiative (k_r) = 0.027 s^{-1} and nonradiative (k_{nr}) = 3.16 s^{-1}.

1.3 Calculation conditions

Density functional theory **(**DFT) calculations (Band gap and DOS calculations) were performed with DMol^3 program [S3,S4]in the Materials Studio 7.0 software package with the generalized gradient approximation with the Perdew-Burke-Ernzerhof functional combined with the TNP basis set. The first Brillouin zone was sampled in the Monkhorst−Pack grid and the 1×8×1 k-points grids were used for the structure optimization and the energy calculations [S5]. The semi-empirical Grimme scheme[S6] for the dispersion correction was included.

The Gibbs free-energy change (ΔG_{ads}) of H intermediate is obtained by calculating the adsorption energy of H, in which 1/2H_2 (g) is used as reference. Besides, the corrections to entropy, zero point energy, and solvation energy are added to the DFT adsorption energy calculations according to the method developed by Nørskov et al. [S7]. Thus, the free energy change of H on the catalyst is defined as follows:

$$\Delta G_{ads} = \Delta E_{ads} + \Delta E_{ZPE} - T\Delta S + \Delta G_S \pm 0.0592\text{pH} \pm \text{eU}$$

where ΔE_{ads} is the adsorption energy of the atomic H on the catalyst, ΔE_{ZPE} is the difference in zero point energy between the adsorbed hydrogen and hydrogen in the gas phase. ΔS is the entropy change of H atom from the absorbed state to the gas phase state. ΔG_S is the solvation energy for reaction intermediate and is set to – 0.22 eV according to previous report [S8]. The pH effect were considered as 0.0592 pH for hydrogen evolution reaction (HER). We set pH 3 in all the calculations due to the pH value of the used aqueous solution of ascorbic acid is about 3. The external potential U was set to 0. Since the H atom is binding on the catalyst surface, the entropy of the adsorbed hydrogen can be negligible. Therefore, the ΔS can be estimated by -1/2×S_0,

in which S_0 is the standard entropy of H_2 with gas phase at pressure of 1 bar and pH = 0 at 300 K. In summary, the Gibbs free-energy change (ΔG_{ads}) of H can be described as

$$\Delta G_{ads} = \Delta E_{ads} + \Delta E_{ZPE} + \Delta G_S + 0.0592pH + 0.0615eV$$

ZPE values could be derived after frequency calculation by [S9]:

$$ZPE = \frac{1}{2}\sum hv_i$$

Synthesis

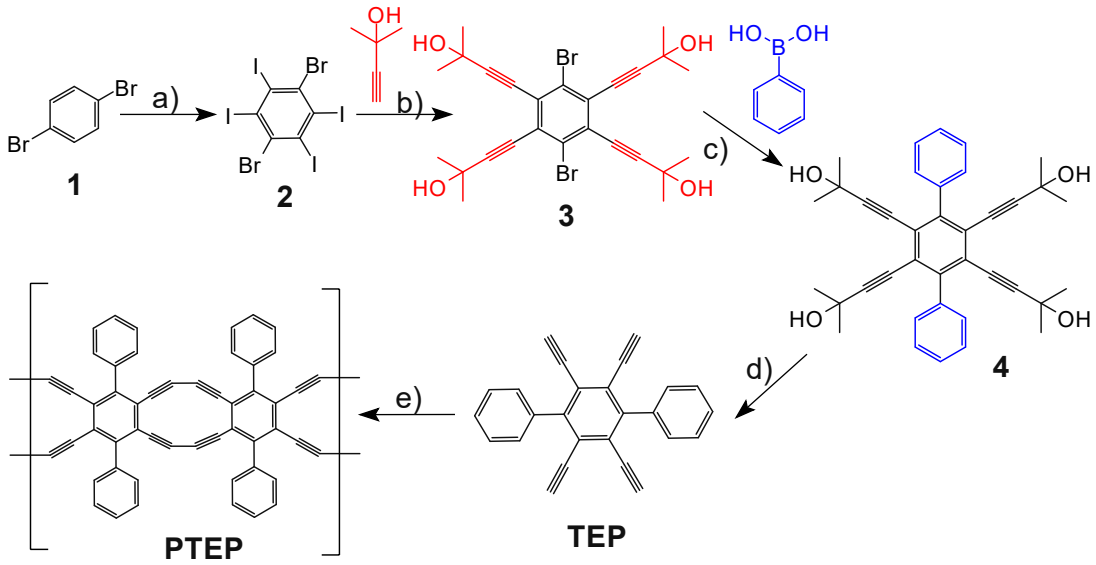

Scheme S1. Synthesis of PTEP. Conditions: (a) I_2, $K_2S_2O_8$, H_2SO_4, TFA, DCE, 80 ℃, 24 h, 80%. (b) 2-Methylbut-3-yn-2-ol, $PdCl_2(PPh)_3$, CuI, TEA, reflux, 20 h, 75%. (c) Phenylboronic acid, $Pd[(PPh)_3]_4$, Toluene/EtOH/H_2O (7/3/2), reflux, 75%. (d) KOH, toluene, 120℃, 15 min, 90%. (e) TMEDA, $CHCl_3$, 120℃, 72 h.

4,4',4'',4'''-(3,6-dibromobenzene-1,2,4,5-tetrayl)tetrakis(2-methylbut-3-yn-2-ol) 3:

[$PdCl_2$ (PPh_3)$_2$] (40 mg) and CuI (20 mg) were added under an argon flow at room temperature to a stirred solution of 1,4-dibromo-2,3,5,6-tetraiodobenzene **2** (3.70 g, 5 mmol) and 2-methylbut-3-yn-2-ol (2.53 g, 30.1 mmol) in TEA. The reaction mixture was then sealed stirred for at 85 °C 24 h, and the mixture was washed with saturated

NH_4Cl and water and then dried over anhydrous Na_2SO_4, then the solvent was removed by evaporation under reduced pressure. The mixture was purified by silica gel chromatography to obtain compound **3** (2.25 g, yield 80%). ^1H NMR (400 MHz, Acetone-d_6) δ 4.67 (s, 4H), 1.61 (s, 24H). ^{13}C NMR (101 MHz, DMSO-d_6) δ 127.95, 127.34, 107.33, 78.87, 64.50, 31.75. MALDI-FTICR-MS (positive): m/z=585.2457, calcd for $C_{26}H_{28}Br_2NaO_4$: m/z=585.0246.

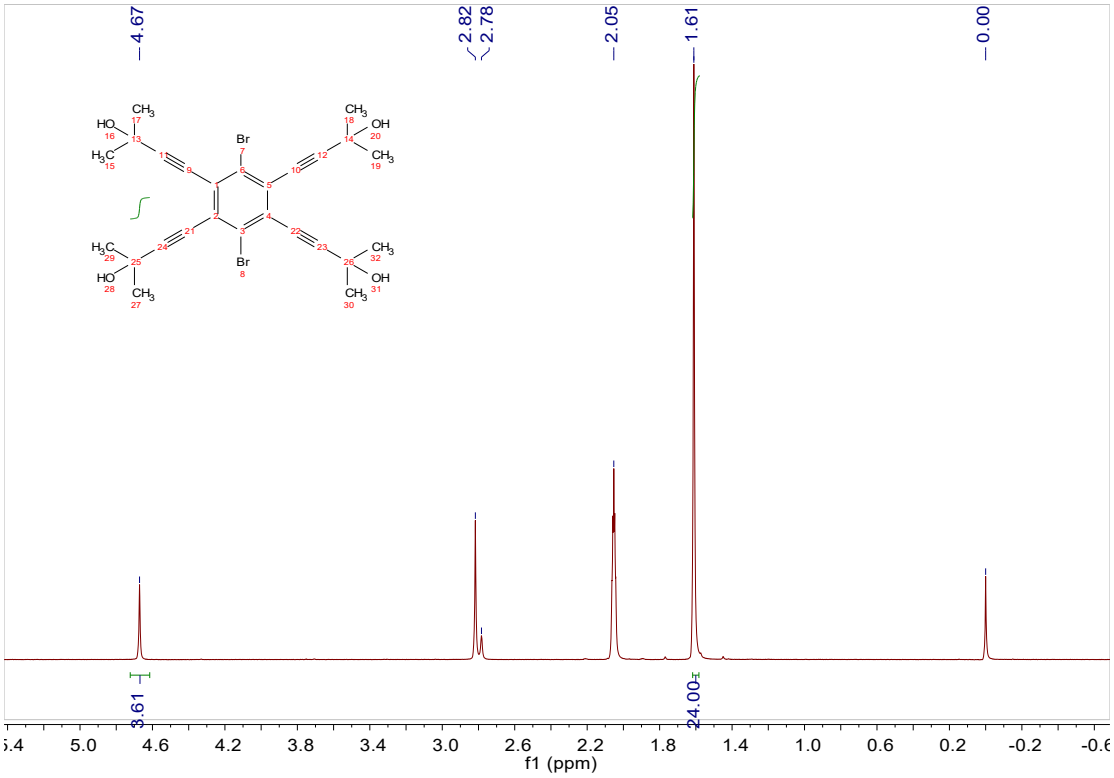

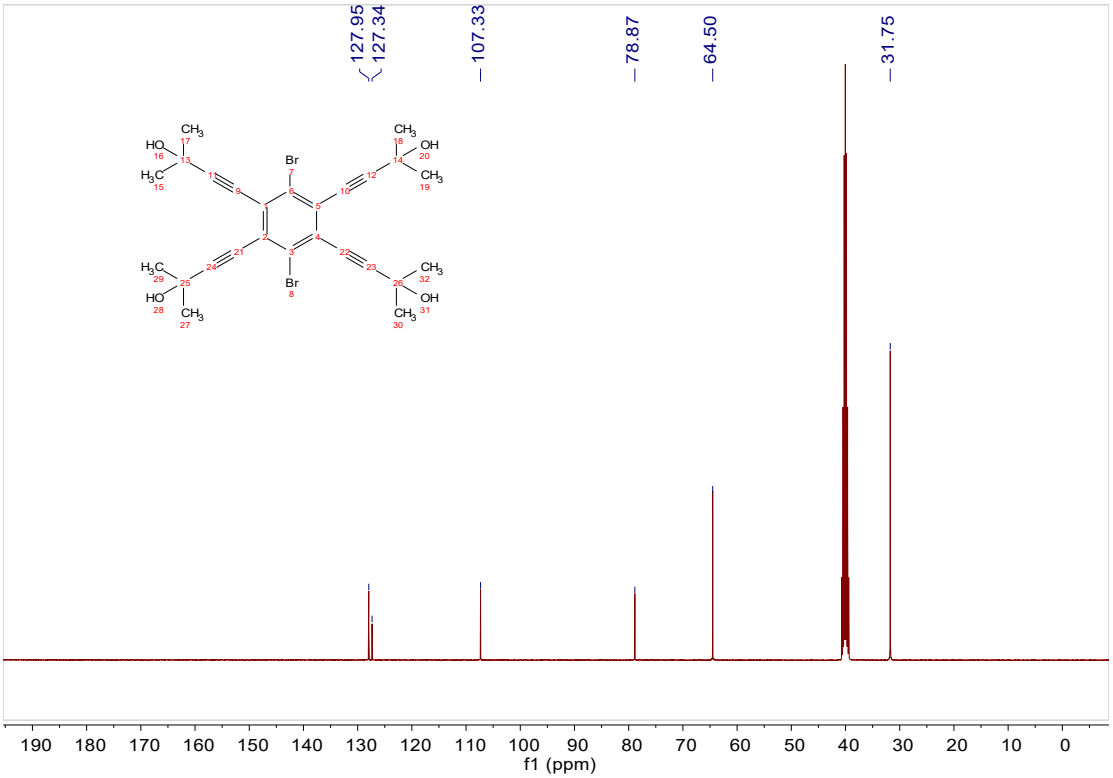

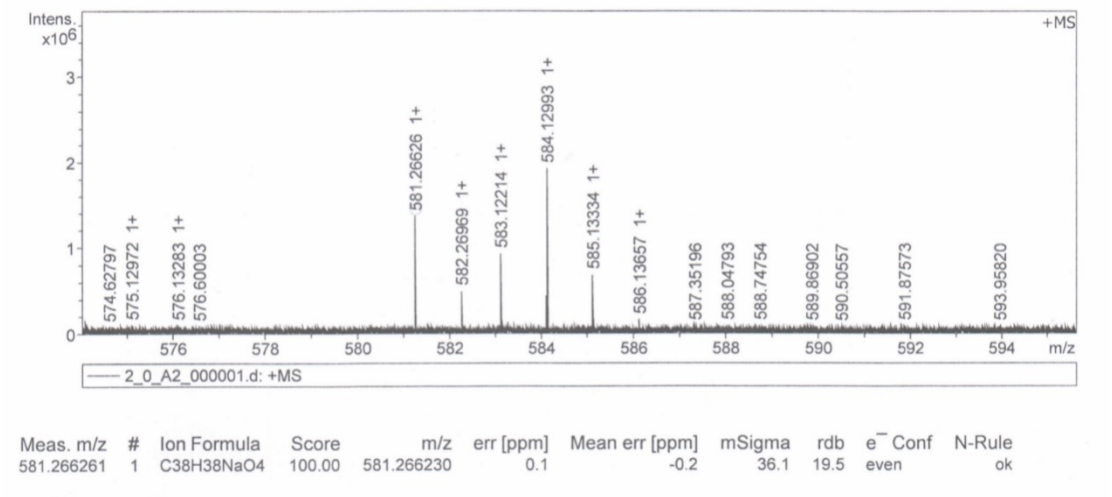

Meas. m/z	#	Ion Formula	Score	m/z	err [ppm]	Mean err [ppm]	mSigma	rdb	e⁻ Conf	N-Rule
581.266261	1	C38H38NaO4	100.00	581.266230	0.1	-0.2	36.1	19.5	even	ok

4,4',4'',4'''-([1,1':4',1''-terphenyl]-2',3',5',6'-tetrayl)tetrakis(2-methylbut-3-yn-2-ol) 4:

[Pd (PPh_3)$_4$] (30 mg), K_2CO_3 (147.5 mg, 1.07mmol) and 2-dicyclohexylphosphino-2',6'-dimethoxybiphenyl (20mg) were added under an argon flow at room temperature to a stirred solution of 4,4',4'',4'''-(3,6-dibromobenzene-1,2,4,5-tetrayl)tetrakis(2-methylbut-3-yn-2-ol) **3** (200 mg, 0.36 mmol) and phenylboronic acid (108.6 mg, 0.89 mmol) in Toluene/EtOH/H_2O (7/3/2 v/v). The reaction mixture was then sealed stirred for at 85 °C 24 h, and the mixture was washed with saturated NH_4Cl and water and then dried over anhydrous Na_2SO_4, then the solvent was removed by evaporation

under reduced pressure. The mixture was purified by silica gel chromatography to obtain compound **4** (140.80 mg, yield 70%). ^{1}H NMR (400 MHz, DMSO-d_6) δ 7.43 (d, J = 5.7 Hz, 4H), 7.41 (s, 4H), 7.39 (d, J = 2.3 Hz, 2H), 5.12 (s, 4H), 1.21 (s, 25H). ^{13}C NMR (101 MHz, DMSO-d_6) δ 145.81, 138.55, 130.21, 128.05, 127.90, 124.91, 104.95, 79.12, 64.13, 31.54. MALDI-FTICR-MS (positive): m/z=581.2662, calcd for $C_{38}H_{38}Br_2O_4$: m/z=581.2662.

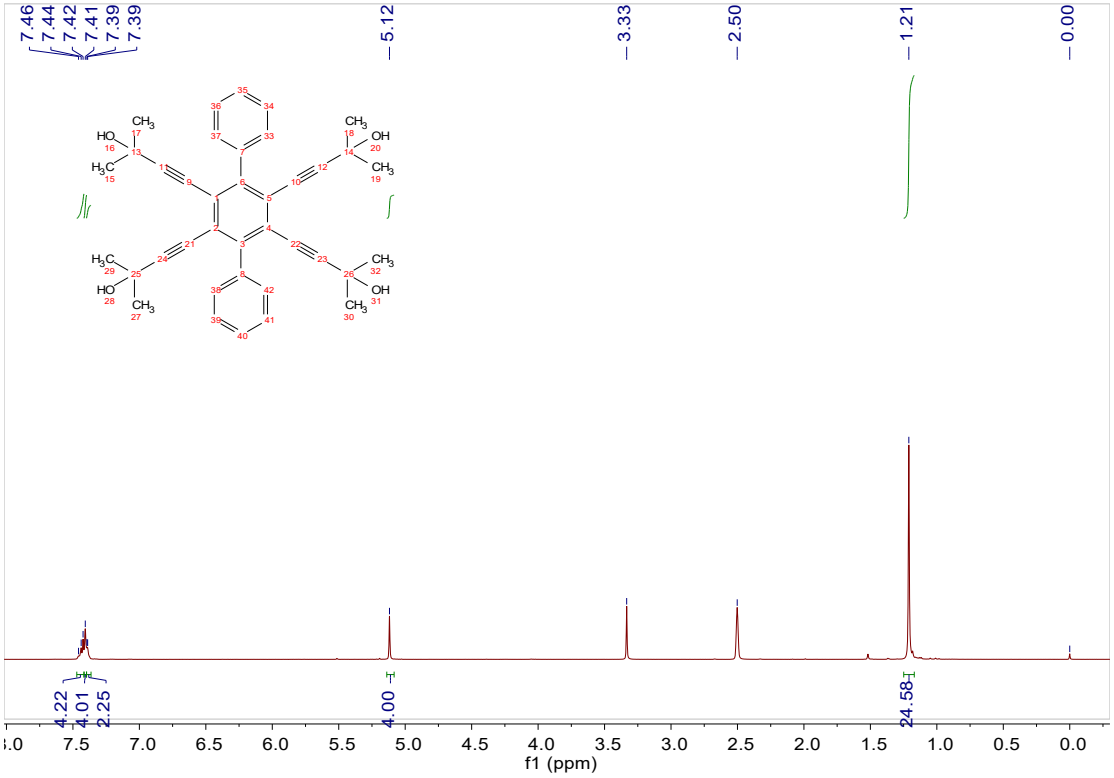

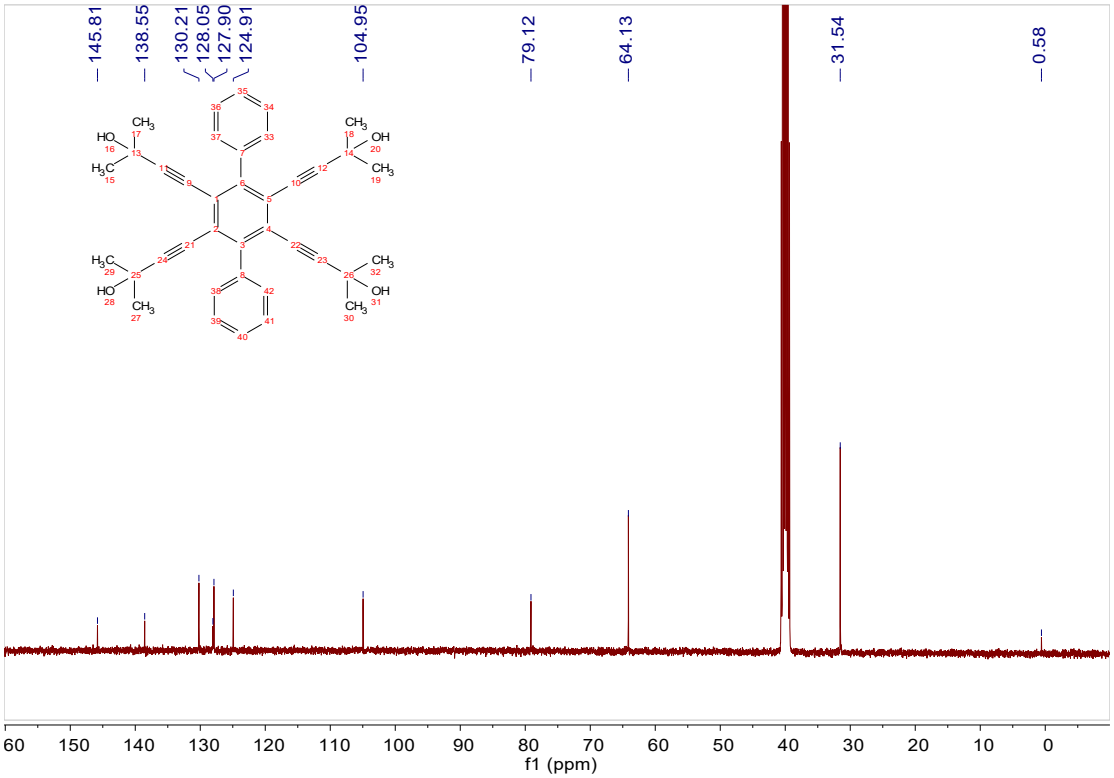

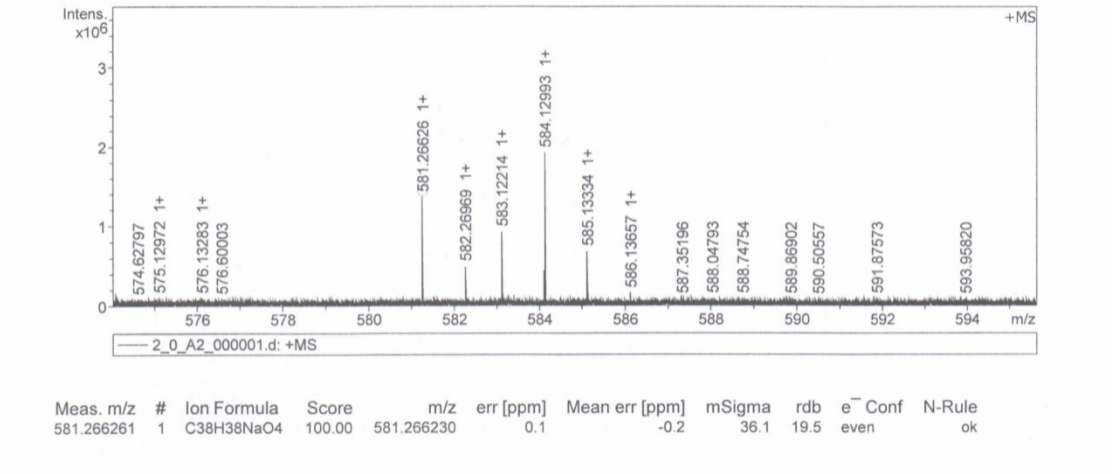

Meas. m/z	#	Ion Formula	Score	m/z	err [ppm]	Mean err [ppm]	mSigma	rdb	e⁻ Conf	N-Rule
581.266261	1	C38H38NaO4	100.00	581.266230	0.1	-0.2	36.1	19.5	even	ok

2',3',5',6'-tetraethynyl-1,1':4',1''-terphenyl (TEP):

Ground KOH (160 mg, 2.56 mmol) was added to compound **4** (200 mg, 0.358 mmol) in toluene which had already been heated to 120°C. The reaction mixture was stirred for 15 minutes. After cooling down to room temperature, water (30 ml) was added to the reaction mixture. The resultant suspension was extracted with dichloromethane (3×50 mL). The combined organic layers were washed with water and then dried over anhydrous Na_2SO_4. The solvent was removed and the crude product was purified by column chromatography (silica gel, petroleum ether) to obtain the desired compound 2',3',5',6'-tetraethynyl-1,1':4',1''-terphenyl **(TEP)** (105.7 mg, 90%).^{1}H NMR (400

MHz, Chloroform-*d*) δ 7.45 (s, 10H), 3.27 (s, 4H). ^{13}C NMR (101 MHz, Chloroform-*d*) δ 147.24, 138.09, 129.63, 128.18, 127.83, 125.56, 86.81, 80.55. MALDI-FTICR-MS (positive): m/z=326.1090, calcd for $C_{26}H_{14}$: m/z=326.1090.

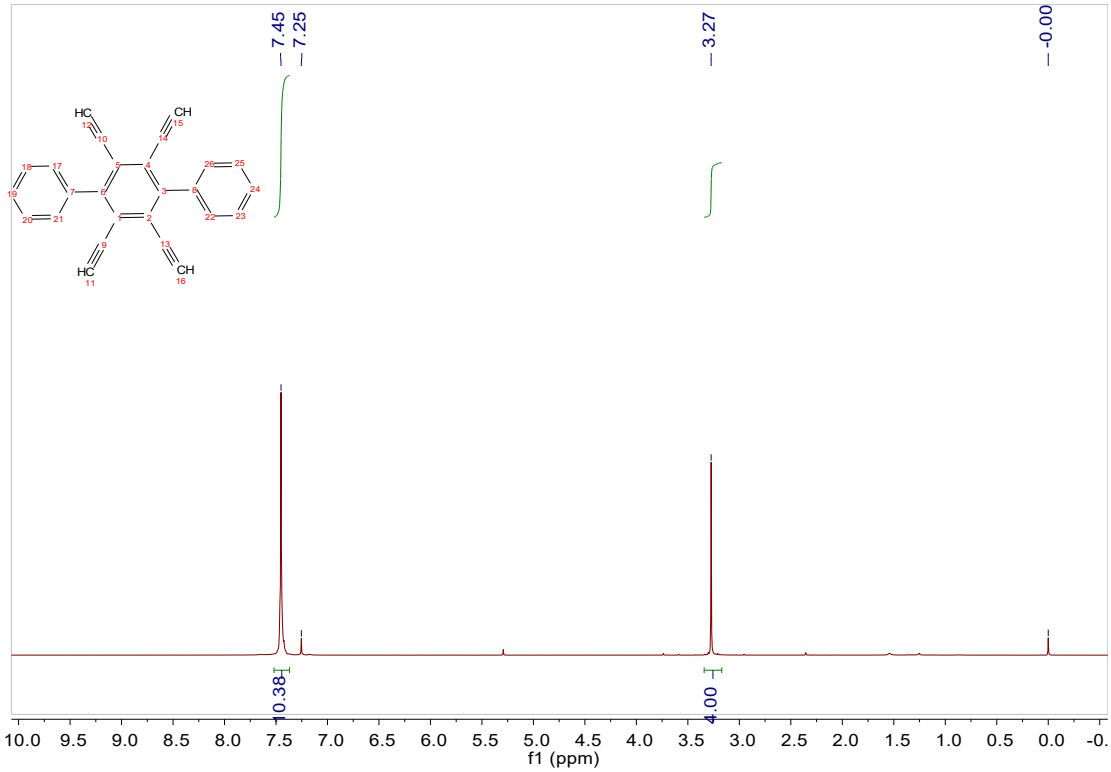

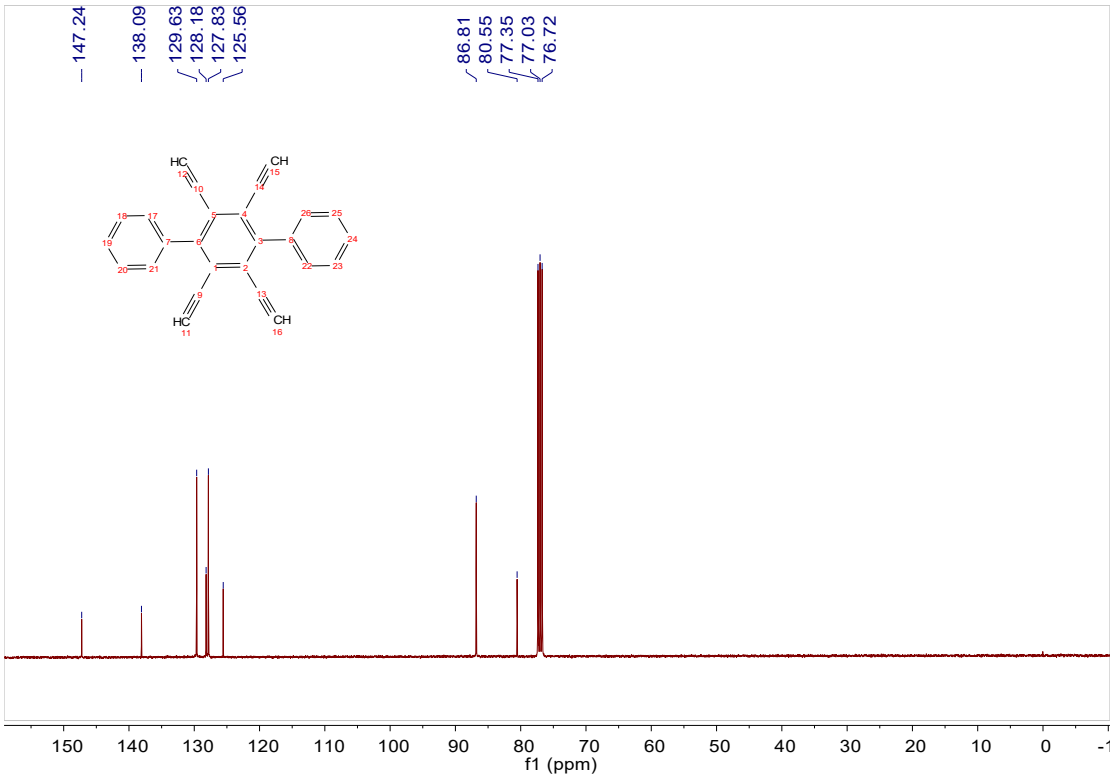

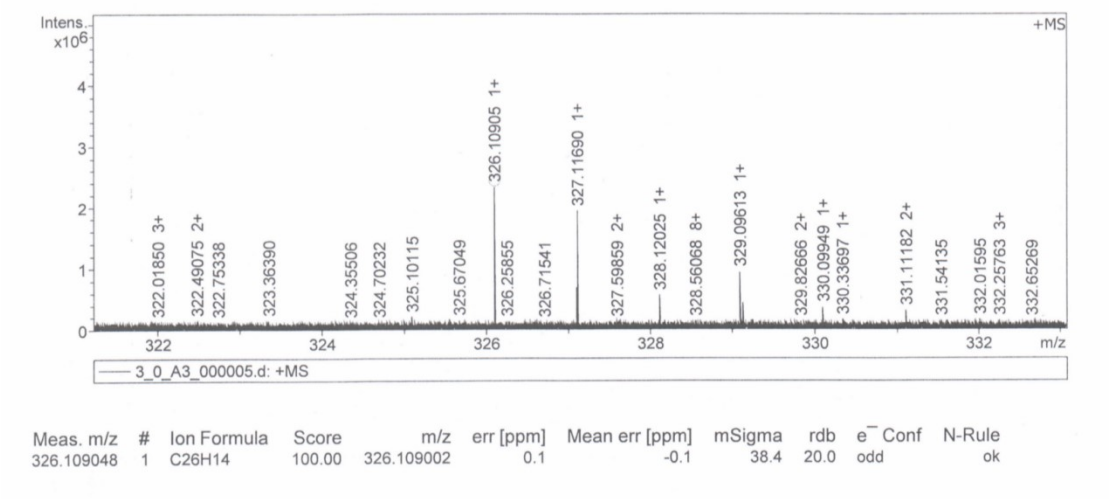

Synthesis of **PTEP**:

The copper sheet was first washed in an ultrasonic bath with a 1 M hydrochloric acid (HCl) solution for 20 minutes. It was then sequentially rinsed with H_2O and acetone, and placed in an argon environment. Next, 10 mg of TEP was dispersed in a mixed solution of chloroform (500 mL) and TMEDA (100 μL), and the copper sheet was added to the mixture. The reaction was carried out at 45 °C in contact with air for 72 hours. After the reaction, the copper sheet was taken out and rinsed with acetone to remove any residual solvent. The washed copper sheet was then immersed in a saturated ammonium persulfate solution. Once no further detachment of solid from the copper surface was observed, the sheet was removed. The resulting filtrate was subjected to suction filtration, and the solid was successively washed with 1 M dilute hydrochloric acid solution, H_2O, and ethanol. After drying, the PTEP product was obtained (7.8mg, 78%).

Synthesis of 1,4-diethynylbenzene (**DEB)**: Synthesis of **DEB** was performed according to literature [S1,S2]. ^{1}H NMR (400 MHz, Chloroform-*d*) δ 7.45 (s, 4H), 3.18 (s, 2H).

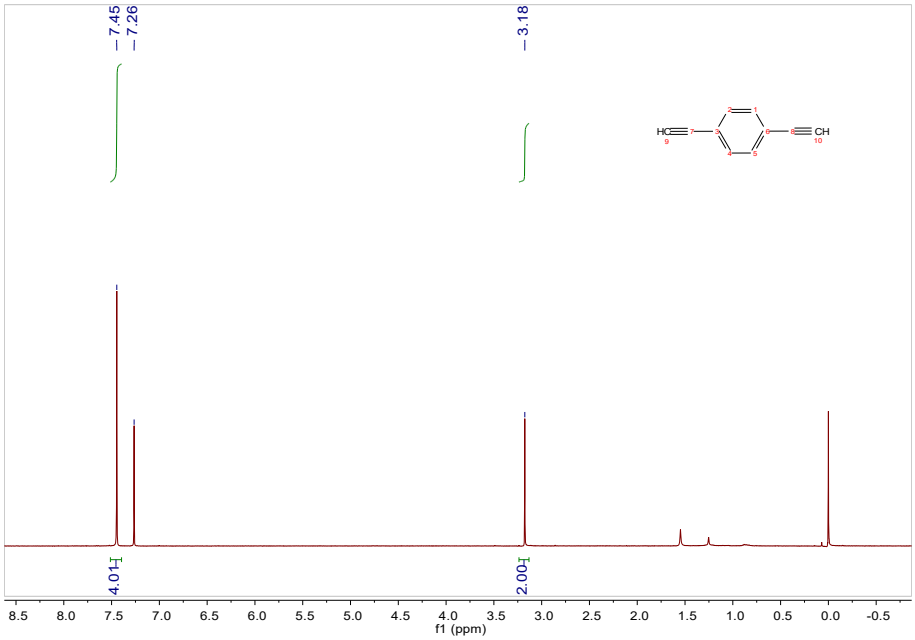

Synthesis of **PDEB**:

The copper sheet was first washed in an ultrasonic bath with a 1 M hydrochloric acid (HCl) solution for 20 minutes. It was then sequentially rinsed with H_2O and acetone, and placed in an argon environment. Next, 10 mg of DEB was dispersed in a mixed solution of chloroform (500 mL) and TMEDA (100 μL), and the copper sheet was added to the mixture. The reaction was carried out at 45 °C in contact with air for 72 hours. After the reaction, the copper sheet was taken out and rinsed with acetone to remove any residual solvent. The washed copper sheet was then immersed in a saturated ammonium persulfate solution. Once no further detachment of solid from the copper surface was observed, the sheet was removed. The resulting filtrate was subjected to suction filtration, and the solid was successively washed with 1 M dilute hydrochloric acid solution, H_2O, and ethanol. After drying, the DEP product was obtained (8.2mg, 82%).

Control experiment to verify the prior formation PTEP

To further verify the structure of PTEP, a small molecule with a structure analogous to TEP, 2',3'-bis((trimethylsilyl)ethynyl)-1,1':4',1"-terphenyl, was synthesized. After removal of the protecting groups, it was grown into dimer and trimer using the exact same method employed for the synthesis of PTEP. The resulting product mixture was roughly separated via silica gel column chromatography to yield a mixture containing the dimer and trimer. Since the NMR spectra of the dimer and trimer each possess their own characteristic peaks (the characteristic peak for the dimer appears at 7.19 ppm corresponding to 4 hydrogen atoms, while the characteristic peaks for the trimer appear at 7.59/7.57 ppm corresponding to a total of 12 hydrogen atoms), the ratio of these two components in the mixture could be determined by integrating the corresponding peak areas in the NMR spectrum. (The dimer, which is the product featuring the curved alkyne structure, accounted for a molar percentage of 90.2%.)

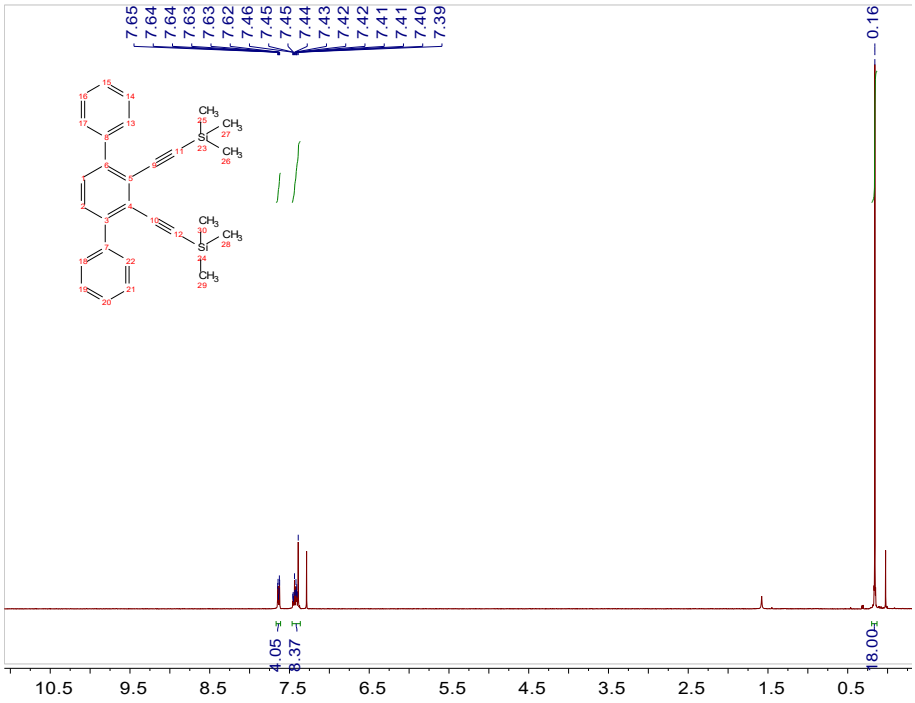

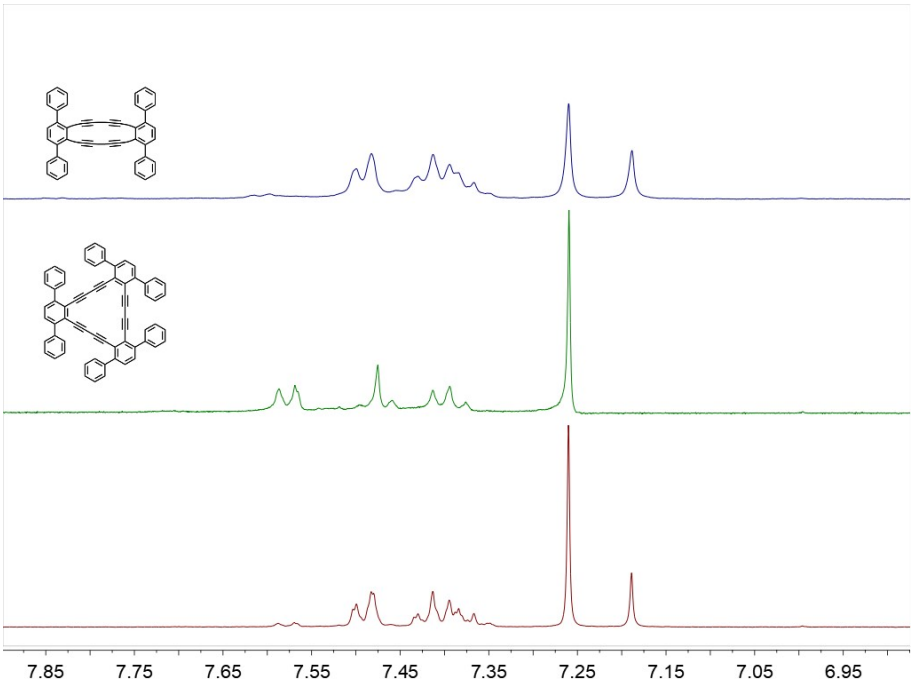

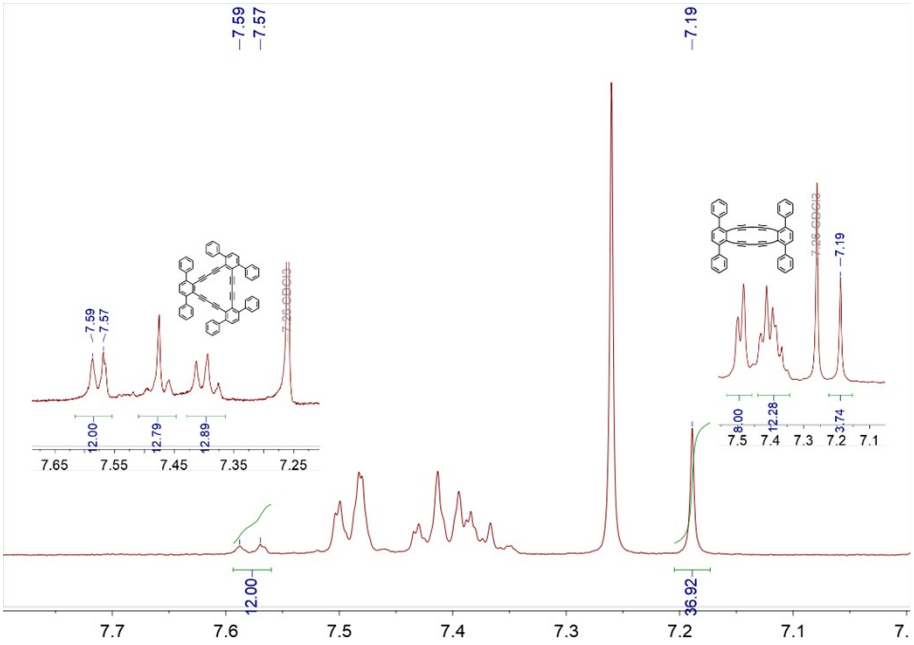

2 X-Ray Diffraction Data Analysis

A suitable crystal of $C_{26}H_{14}$ was selected and mounted on a XtaLAB Synergy R, HyPix diffractometer. The crystal was kept at 170.00(10) during data collection. Using Olex2 [S10], the structure was solved with the olex2.solve [S11] structure solution program using Charge Flipping and refined with the SHELXL [S12] refinement package using Least Squares minimisation. Accession codes: The X-ray

crystallographic coordinates for structure reported in this article have been deposited at the Cambridge Crystallographic Data Centre (CCDC), under deposition number CCDC 2513878. These data can be obtained free of charge from CCDC via http://www.ccdc.cam.ac.uk/data_request/cif.

Crystal structure determination of TEP

Crystal Data for $C_{26}H_{14}$ (M =326.37 g/mol): monoclinic, space group $P2_1/c$ (no. 14), a = 7.11273(15) Å, b = 18.8816(4) Å, c = 6.81150(14) Å, β = 91.315(2)°, V = 914.54(3) Å^3, Z = 2, T = 170.00(10) K, μ(Cu Kα) = 0.513 mm^{-1}, *Dcalc* = 1.185 g/cm^3, 5917 reflections measured (9.368° ≤ 2Θ ≤ 151.626°), 1826 unique (R_{int} = 0.0225, R_{sigma} = 0.0223) which were used in all calculations. The final R_1 was 0.0347 (I > 2σ(I)) and wR_2 was 0.0969 (all data).

Table S1 Crystal data and structure refinement for **TEP**.

Identification code	**TEP**
Empirical formula	$C_{26}H_{14}$
Formula weight	326.37
Temperature/K	170.00(10)
Crystal system	monoclinic
Space group	$P2_1/c$
a/Å	7.11273(15)
b/Å	18.8816(4)
c/Å	6.81150(14)
α/°	90
β/°	91.315(2)
γ/°	90
Volume/Å^3	914.54(3)
Z	2
ρ_{calc}g/cm^3	1.185
μ/mm^{-1}	0.513
F(000)	340.0
Crystal size/mm^3	0.3 × 0.2 × 0.1
Radiation	CuKα (λ = 1.54184)
2θ range for data collection/°	9.368 to 151.626
Index ranges	-8 ≤ h ≤ 8, -9 ≤ k ≤ 23, -8 ≤ l ≤ 7
Reflections collected	5917

Independent reflections	1826 [R_{int} = 0.0225, R_{sigma} = 0.0223]
Data/restraints/parameters	1826/0/119
Goodness-of-fit on F^2	1.087
Final R indexes [I>=2σ (I)]	R_1 = 0.0347, wR_2 = 0.0946
Final R indexes [all data]	R_1 = 0.0376, wR_2 = 0.0969
Largest diff. peak/hole / e $Å^{-3}$	0.19/-0.11

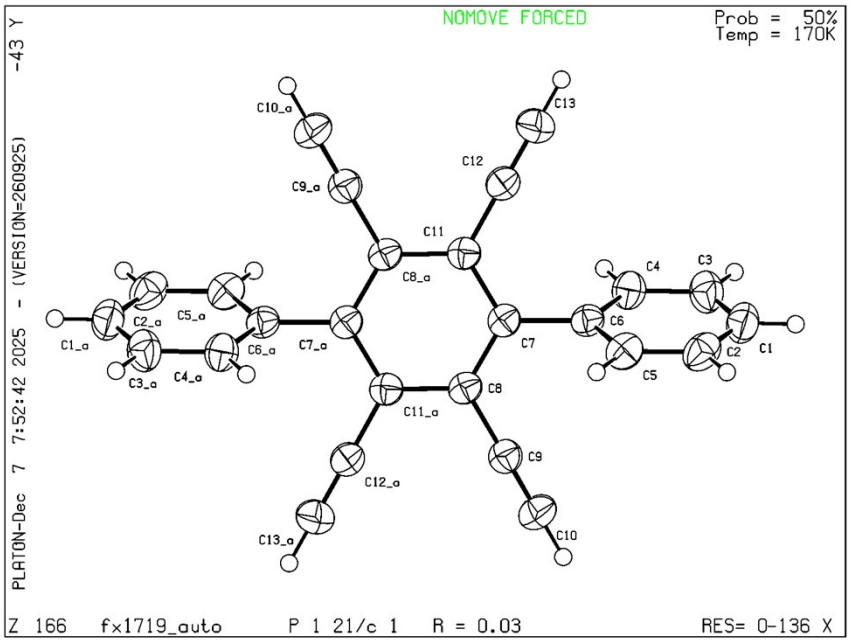

Figure S1. Dispersion of **PTEP** in water after ultrasonication for 15 minutes.

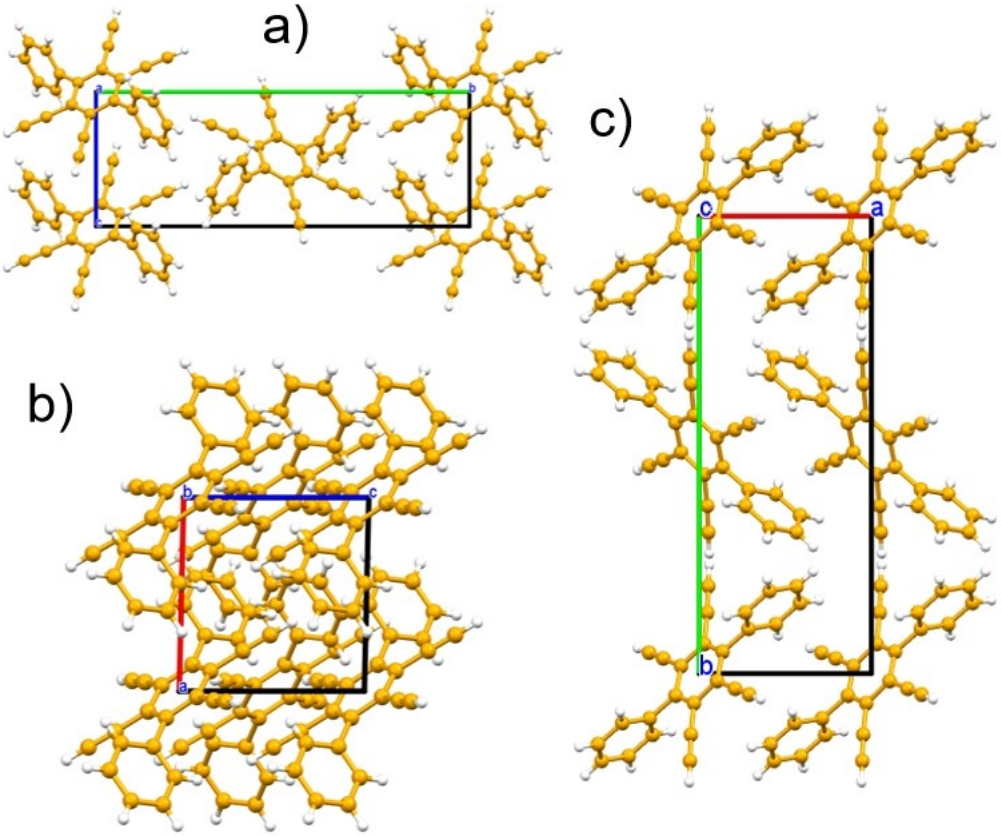

Figure S2. Crystal packing of **TEP**. Views along the a, b and axis.

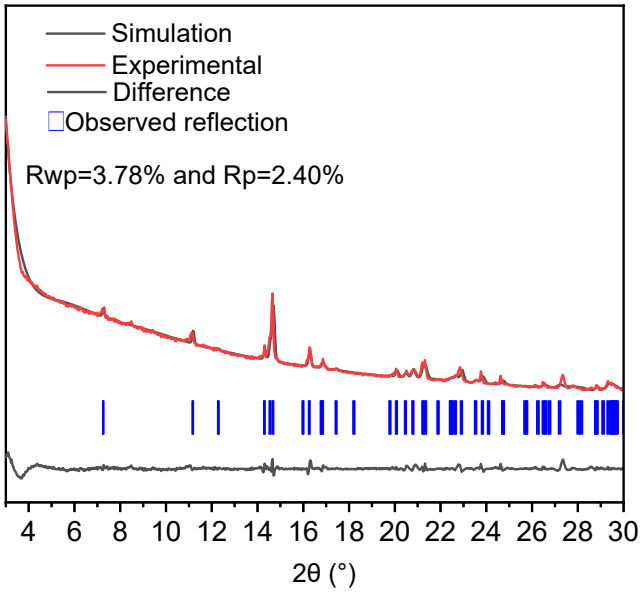

Figure S3. Experimental and simulated PXRD patterns of **PTEP**.

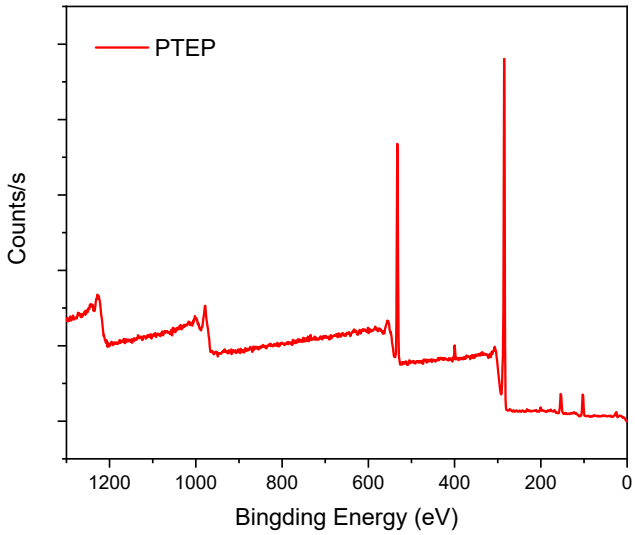

Figure S4. XPS survey spectra of **PTEP**.

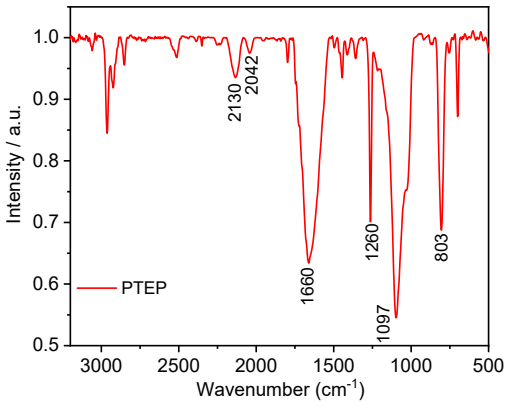

Figure S5. FTIR spectra of PTEP, the disappearance of the terminal alkyne C-H stretch and the C≡C stretch confirmed the formation of **PTEP**.

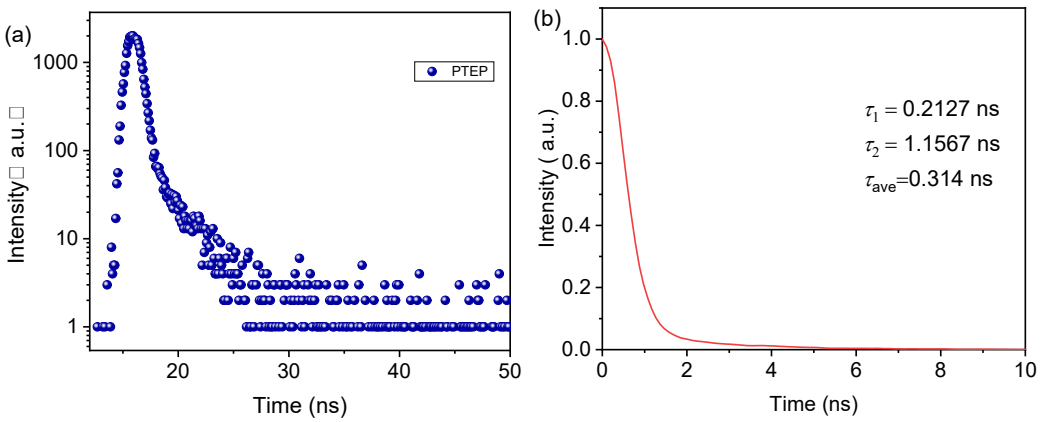

Figure S6. (a) TRPL decay spectra and (b) corresponding fitting result of TRPL decay curve of **PTEP**.

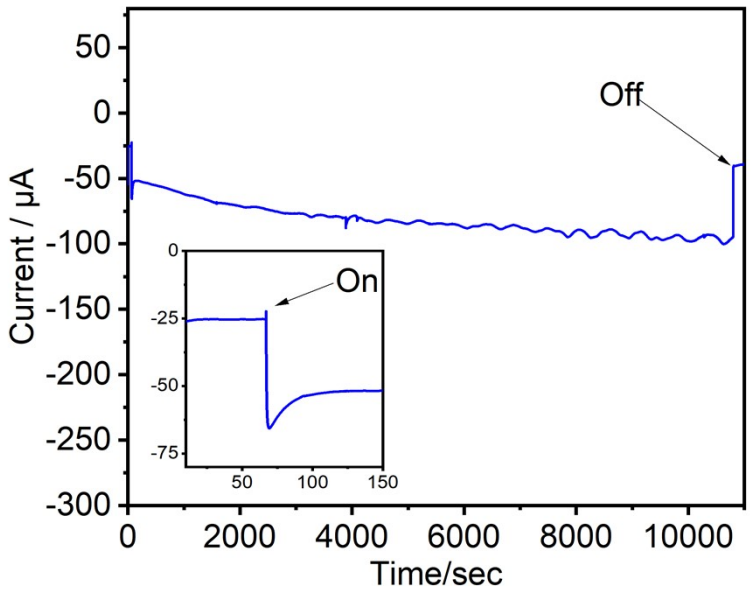

Figure S7. Current density vs. time of the **PTEP** electrode under illumination for 10800s. Inset: magnification of 10–150s.

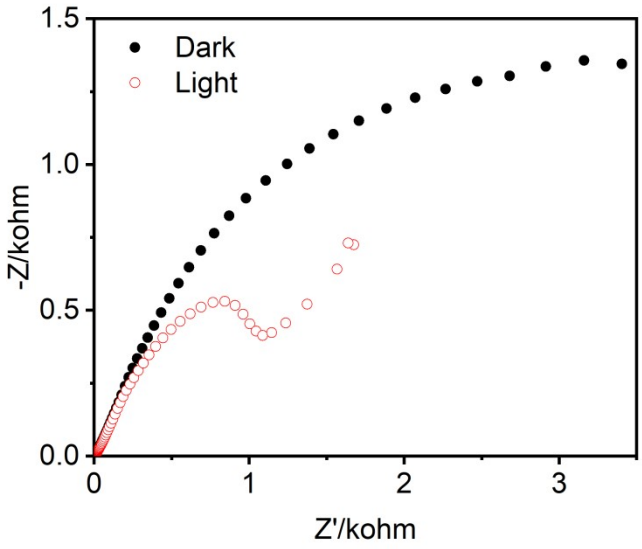

Figure S8. EIS (recorded at 0.30 V vs. RHE) of **PTEP** under light or in the dark: after long time irradiation.

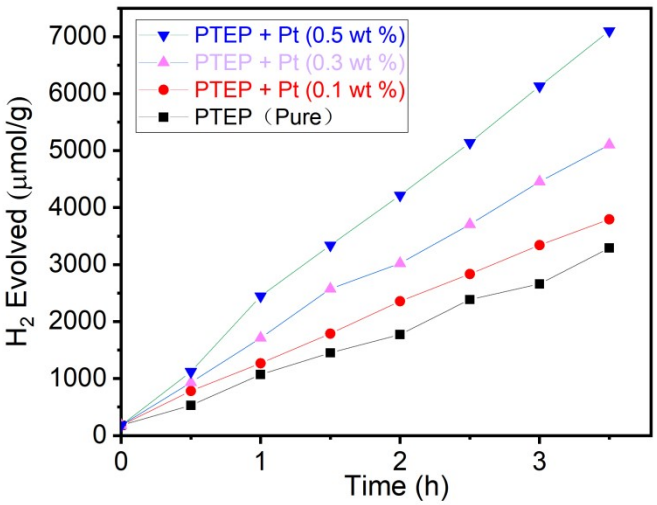

Figure S9. Photocatalytic H_2 evolution rates of PTEP with different Pt loadings.

Figure S10. Post-reaction characterization of **PTEP**: TEM image showing well-dispersed Pt nanoparticles on **PTEP**.

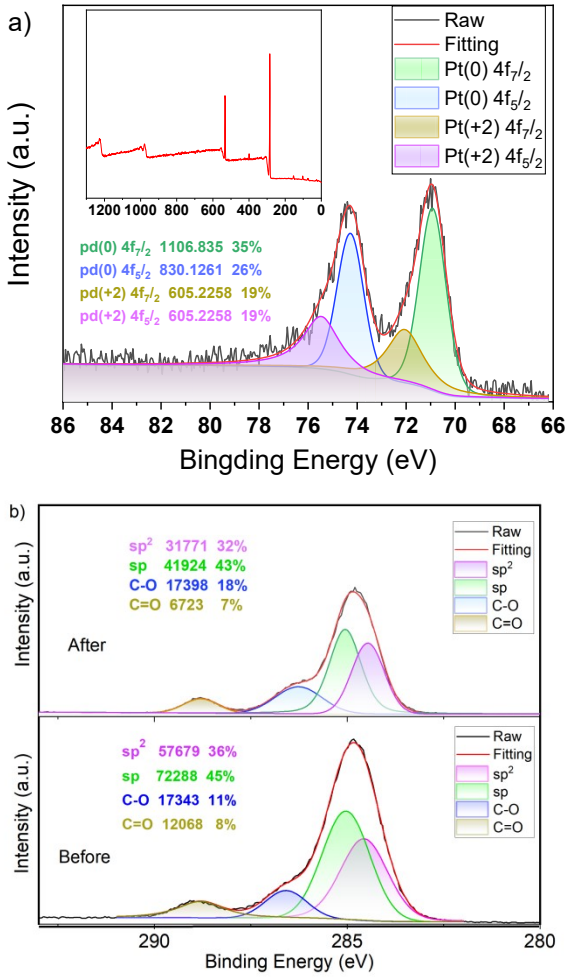

Figure S11. XPS spectra after photoelectrochemical experiments: a) Pt existed as Pt(2+) (38%) and Pt(0) (62%); b) C1s before and after hydrogen evolution, showed little increasing of C-O and C=O signals, indicating good stability of PTEP.

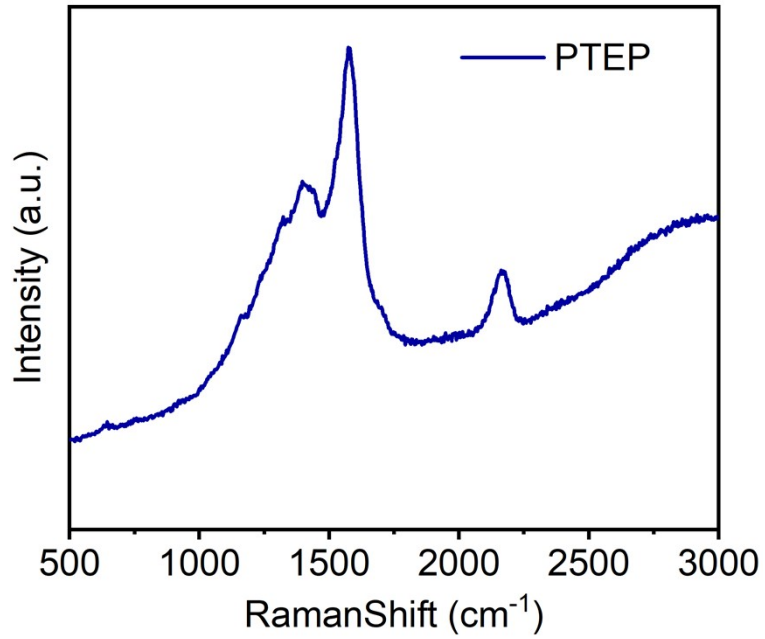

Figure S12. Raman spectra of **PTEP** after recycling experiments for H_2 production under visible light irradiation (λ＞420 nm).

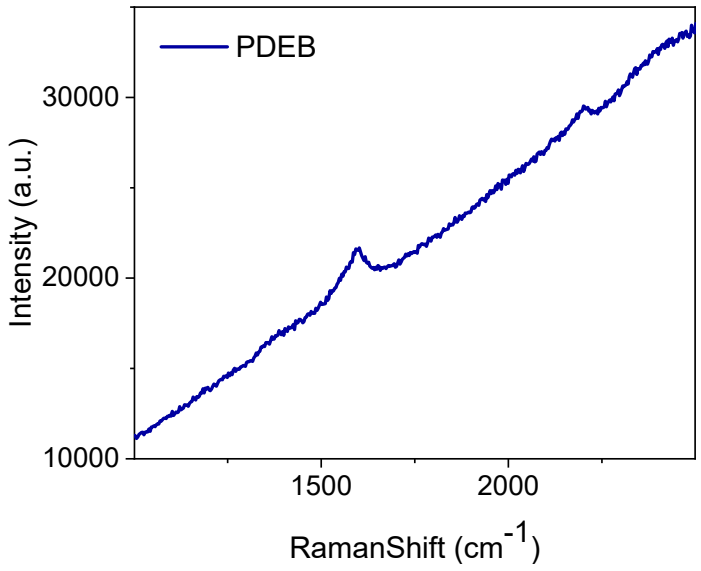

Figure S13. Raman spectrum of **PDEB**. The characteristic peak of the benzene ring at around 1600 cm^{-1} and the peak attributed to the alkyne bond at around 2200 cm^{-1} can be clearly observed.

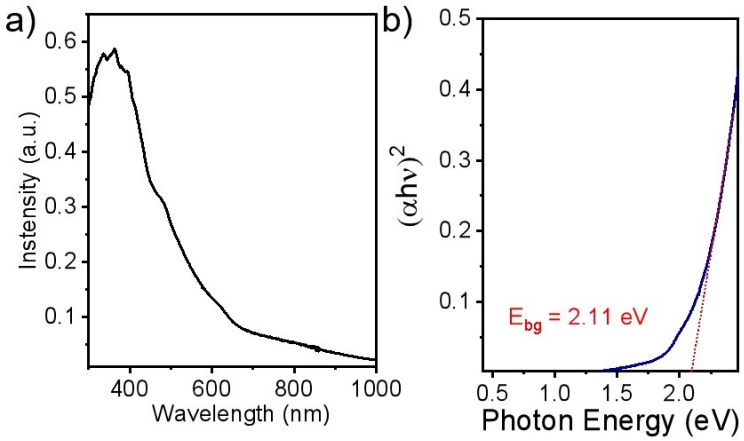

Figure S14. a) UV-Vis DRS spectra of PDEB; b) $(\alpha h\nu)^2$ versus hν curve of **PDEB**.

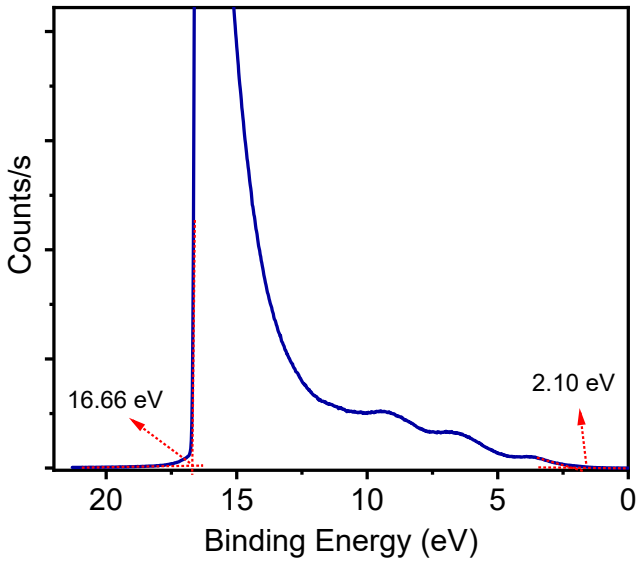

Figure S15. UPS spectrum of **PDEB** (black curve). The dashed red lines mark the baseline and the tangents of the curve. The edges of the UPS spectrum are given by the intersections of two dashed red lines of the tangents and the baseline, from which the UPS width is determined.

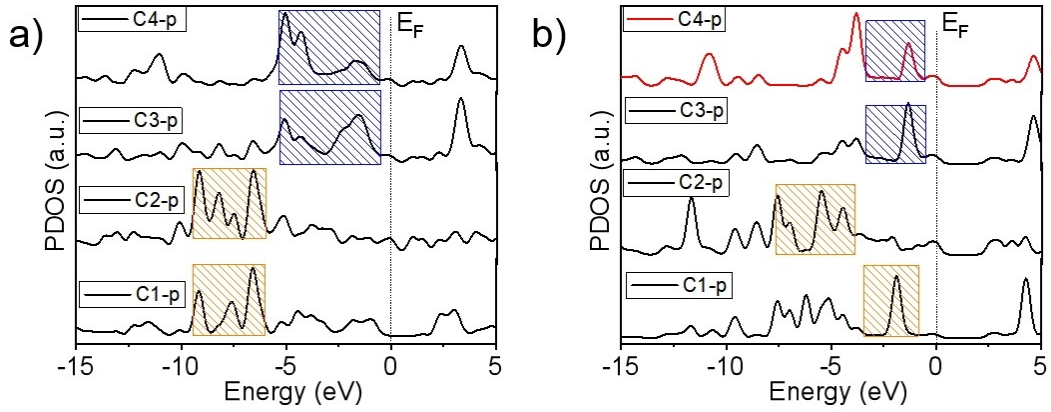

Figure S16. The PDOS of p-orbitals for four different typical C-sites within the **PTEP** (a) and **PDEB** (b) system.

Figure S17. BET data of **PTEP** and **PDEB**: the specific surface area of **PTEP** is approximately 280.5 m^2/g with a pore size of about 1.26 nm, while the specific surface area of **PDEB** could not be detected.

Table S3. Comparison of photocatalytic hydrogen evolution performance of **PTEP** with representative graphdiyne-based and g-C_3N_4-based photocatalysts.

Photocatalyst	**Cocatalyst**	**Light Source**	**Sacrificial reagent**	**HER (μmol g^{-1} h^{-1})**	**AQY (%) @ λ (nm)**	**Stability**	**Band Gap (eV)**	**Ref.**
PTEP (This Work)	**Pt**	**λ≥ 420 nm**	**ascorbic acid**	**>2250**	**8.0% @ 420 nm**	**>21 h stable**	**1.61**	**This work**
g-C_3N_4 (nitrogen	Pt	λ ≥ 420	TEOA	1632	7.5% @	5 cycles	2.85	[S13]

vacancy engineered)		nm			450 nm	stable		
Ag/TCN (tubular g-C_3N_4)	Ag	λ ≥ 420 nm	TEOA	2667	7.12% @ 420 nm	3 cycles stable	2.80	[S14]
Ni-Co_3O_4-C_3N_4	Ni/Co_3O_4	λ ≥ 420 nm	TEOA	1671 (μmol h^{-1}, total)	6.2 % @ 400 nm	Good	n.r.	[S15]
g-C_3N_4 (pristine)	–	λ ≥ 420 nm	TEOA	~120–327	<5%	Moderate	~2.7	[S15]
g-C_3N_4/GDY	Pt	Xe arc lamp, 300W	TEOA	454.28 μmol/h	n.r.	5 cycles stable	n.r.	[S16]
GDY/g-C_3N_4	Pt	350 W Xe lamp (λ > 420 nm)	TEOA	39.6 μmol/h	n.r.	>12 h stable	2.8	[S17]
$CuCo_2O_4$/GDY/CuO	-	Xe lamp, 300 W	Na_2S/Na_2SO_3	9617 μmol/g/h	10.29% at 360 nm	>30 h stable	1.74	[S18]
g-C_3N_4/Co_3S_4@S,N-GDY	-	LED light, 5 W(λ > 420 nm)	TEOA	2075.67 μmol/g/h	2.10% at 400 nm	Good	1.62	[S19]
NiBi/GDY	-	Xe lamp, 300 W	TEOA	4.54 mmol/g/h	~1.75% at 525 nm	>35 h stable	n.r.	[S20]
CdS/GDY	-	450 nm LED, 200 mW cm^{-2}	TEOA	410 μmol/g/h	n.r.	>12 h stable	n.r.	[S21]

n.r. = not reported.

Reference:

[S1] Reddy, C. M.; Kirchner, M. T.; Gundakaram, R. C.; Padmanabhan, K. A.; Desiraju, G. R., *Chem. Eur. J.***2006**, 12(8), 2222–2234.

[S2] Shu, W.; Guan, C.; Guo, W.; Wang, C.; Shen, Y., *J. Mater. Chem.***2012**, 22(7), 3075–3081.

[S3] B. Delley, *J. Chem. Phys.* **1990**, 92, 508–517.

[S4] B. Delley, *J. Chem. Phys.* **2000**, 113, 7756–7764.

[S5] H. J. Monkhorst, J. D. Pack, *Phys. Rev. B* **1976**, 13, 5188-5192.

[S6] S. Grimme, *J. Comput. Chem.* **2006**, 27, 1787–1799.

[S7] J. K. Nørskov, J. Rossmeisl, A. Logadottir, L. Lindqvist, *J. Phys. Chem. B* **2004**, 108, 17886–17892.

[S8] T. Zhang, Y. Hou, V. Dzhagan, Z. Liao, G. Chai, M. Loeffler, D. Olianas, A. Milani, S. Xu, M. Tommasini, D. R. T. Zahn, Z. Zheng, E. Zschech, R. Jordan, X. Feng, *Nat. Commun.* **2018**, 9, 1140.

[S9] J. K. Nørskov, J. Rossmeisl, A. Logadottir, L. Lindqvist, J. R. Kitchin, T. Bligaard, H. Jónsson, *J. Chem. Phys. B* **2004**, 108, 17886-17892.
[S10] O.V. Dolomanov, L.J. Bourhis, R.J. Gildea, J.A.K. Howard, H., J. *Puschmann, Appl. Cryst*. **2009**, 42, 339-341.
[S11] L.J. Bourhis, O.V. Dolomanov, R.J. Gildea, J.A.K. Howard, H. Puschmann, *Acta Cryst*. **2015**, A71, 59-75.
[S12] G.M. Sheldrick, *Acta Cryst*. **2015**, C71, 3-8.
[S13] I. U., J.-H. Li, S. Chen, M. Amin, P. Zhao, N. Qin, and A.-W. Xu, *ACS Appl. Nano Mater.* **2025**, 8, 12111−12118.
[S14] Y. Huang, Z.J. Si, T. Ding, K. Zhou, Z. Nie, Y. Zeng, *Environ. Res.,* **2025**, 285, 122332.
[S15] Y.M. Zhang , Y.P. Zhang, J.G. Yang, C.C. Feng, S.B. Shao, P.S. Li, Q.Z. Dong, X.S. Wang, *J. Catal.,* **2025**, 450, 116296.
[S16] H.Y. S, Q.X. Deng, C. Yin , J.Y. Zhou , S.Q. Zhang , Y.X. Zhang , Z.C. Liu, J.B. Zhang, J. Zhang, J. Kong, *J. Alloys Comp* **2020**, 833, 155054.
[S17] Q.L. Xu, B.C. Zhu, B. Cheng, J.G. Yu, M.H. Zhou, W.K. Ho, *Appl. Catal. B:* **2019**, 255, 117770.
[S18] K.W.Wang, Z.P. Huang, J. Wang, *Chem. Eng. J.* **2022**, 430, 132727.
[S19] K.C. Yang, T.X. Liu, D.Z. Xiang, Y.J. Li, Z.L. Jin, *Sep. Pur. Tech.* **2022**, 298, 121564.
[S20] X.-P. Yin, S.-W. Luo, S.-F. Tang, X.-L. Lu, Tong-Bu Lu, *Chinese J. Catal.* **2021**, 42 , 1379–1386
[S21] J.-X. Lv, Z.-M. Zhang, J. Wang, X.-L. Lu, W. Zhang, and T.-B. Lu, *ACS Appl. Mater. Interfaces* **2019**, 11, 2655−2661.